Measurement-Based Characterization of Residual Self-Interference on a Full-Duplex MIMO Testbed

Konstantinos Alexandris, Alexios Balatsoukas-Stimming, and Andreas Burg
Telecommunications Circuits Laboratory,
École Polytechnique Fédérale de Lausanne, Switzerland

***Abstract*—Full-duplex communication systems require very strong self-interference suppression. Unfortunately, perfect suppression is not possible in practice and some residual self-interference remains. This residual self-interference acts as additive noise whose statistical properties may be different from those of thermal noise. This work presents a measurement-based study of the statistical properties of residual self-interference on an OFDM based full-duplex MIMO testbed. Moreover, we quantify the effect that residual self-interference has on some popular MIMO receivers and we employ a strategy to reduce the performance impact of residual-self interference.**

I. Introduction

True full-duplex (FD) wireless communication [1] has recently re-attracted significant attention. In FD systems the strong self-interference which is present needs to be suppressed, ideally to the level of the thermal noise floor. Suppression can be achieved by passive means or by active injection of a cancelation signal. One can generate a cancelation signal directly in the analog domain [2] or in the digital domain [3]. This second approach provides slightly worse performance than the first approach, but it is more suitable for full-duplex MIMO (FD-MIMO) applications [4]. The suppression method proposed in [3] is limited by transmitter imperfections [5]. Thus, there is a small residual self-interference signal, containing mainly these imperfections, which the receiver sees as additive noise. The performance of MIMO receivers with transmitter-signal distortions that are similar to those causing the residual self-interference in FD-MIMO was studied in [6]. An i.i.d. Gaussian assumption is used in [6] to model the imperfections in a MIMO-OFDM context. However, it is not obvious that the same model can be used for the residual self-interference in FD-MIMO systems and more sophisticated models have already been studied [7], [8].

Contribution: In this work, we measure the residual self-interference both in the time domain and in the frequency domain on an FD-MIMO testbed and we make a first step towards its modeling. Moreover, we study the effect of residual self-interference on two well-known MIMO receivers through MATLAB simulations which use measured noise samples from our testbed.

II. MIMO Receivers and Full-Duplex MIMO

A. MIMO Receivers

Consider an $M \times M$ MIMO node which is receiving a signal $\mathbf{x} \in \mathcal{O}^M$ over a channel $\mathbf{H}$, where $\mathcal{O}$ denotes the set of constellation points and $\mathbb{E}[\mathbf{x}\mathbf{x}^H] = \mathbf{I}_M$. The discrete time complex baseband input-output relation is $\mathbf{y} = \mathbf{H}\mathbf{x}+\mathbf{n}_\mathrm{r}$, where $\mathbf{n}_\mathrm{r} \sim \mathcal{CN}(\mathbf{0}, \sigma_\mathrm{r}^2\mathbf{I}_M)$ denotes the thermal noise at the receiver.

1) ZF receiver: The ZF detection algorithm tries to undo the effect of the channel $\mathbf{H}$ by multiplying the received vector $\mathbf{y}$ with the inverse channel matrix $\mathbf{H}^{-1}$. The result is then demapped to the nearest constellation point according to

$$\hat{\mathbf{x}}^{\mathrm{ZF}} = D\left(\mathbf{H}^{-1}\mathbf{y}\right), \tag{1}$$

where $D(\cdot)$ denotes the component-wise scalar ML detector.

2) ML receiver: Under complex normal i.i.d. noise, ML detection reduces to the nearest neighbor rule, i.e.,

$$\hat{\mathbf{x}}^{\mathrm{ML}} = \arg\min_{\mathbf{x}\in\mathcal{O}^M} \|\mathbf{y} - \mathbf{H}\mathbf{x}\|. \tag{2}$$

B. Full-duplex MIMO

An OFDM FD-MIMO node is receiving a signal from a remote node, denoted by $\mathbf{x}$, over a channel $\mathbf{H}$, while *at the same time* transmitting its own signal $\mathbf{x}_\mathrm{t} \in \mathcal{O}^M$, where $\mathcal{O}$ denotes the set of constellation points and $\mathbb{E}[\mathbf{x}_\mathrm{t}\mathbf{x}_\mathrm{t}^H] = \mathbf{I}_M$. The node receives its own transmission through the self-interference channel $\mathbf{H}_\mathrm{t}$. Without active self-interference cancelation the complex baseband input-output relation is

$$\mathbf{y} = \mathbf{H}\mathbf{x} + \mathbf{H}_\mathrm{t}\mathbf{x}_\mathrm{t} + \mathbf{n}_\mathrm{r}. \tag{3}$$

In order to perform active cancelation, the cancelation signal $\mathbf{x}_\mathrm{c}$ is constructed in the complex baseband domain so that $\mathbf{H}_\mathrm{c}\mathbf{x}_\mathrm{c} = -\mathbf{H}_\mathrm{t}\mathbf{x}_\mathrm{t}$, and it is upconverted using a second set of RF chains and added to the received RF signal. Moreover, we consider the case where both $\mathbf{x}_\mathrm{t}$ and $\mathbf{x}_\mathrm{c}$ are distorted due to transmitter imperfections. As in [7], [8], we model these imperfections as additive noise in the complex baseband, so that the impaired signals, denoted by $\tilde{\mathbf{x}}_\mathrm{t}$ and $\tilde{\mathbf{x}}_\mathrm{c}$, respectively, are given by

$$\tilde{\mathbf{x}}_\mathrm{t} = \mathbf{x}_\mathrm{t} + \mathbf{n}_\mathrm{t}, \qquad \tilde{\mathbf{x}}_\mathrm{c} = \mathbf{x}_\mathrm{c} + \mathbf{n}_\mathrm{c}. \tag{4}$$

Thus, when cancelation is performed and in the presence of transmitter impairments, we have

$$\mathbf{y} = \mathbf{H}\mathbf{x} + \mathbf{H}_\mathrm{t}\tilde{\mathbf{x}}_\mathrm{t} + \mathbf{H}_\mathrm{c}\tilde{\mathbf{x}}_\mathrm{c} + \mathbf{n}_\mathrm{r} \tag{5}$$

$$= \mathbf{H}\mathbf{x} + \mathbf{H}_\mathrm{t}\mathbf{n}_\mathrm{t} + \mathbf{H}_\mathrm{c}\mathbf{n}_\mathrm{c} + \mathbf{n}_\mathrm{r}. \tag{6}$$

We define the *effective noise* as

$$\mathbf{n}_\mathrm{eff} \triangleq \mathbf{H}_\mathrm{t}\mathbf{n}_\mathrm{t} + \mathbf{H}_\mathrm{c}\mathbf{n}_\mathrm{c} + \mathbf{n}_\mathrm{r}, \tag{7}$$

which leads to $\mathbf{y} = \mathbf{H}\mathbf{x} + \mathbf{n}_\mathrm{eff}$. For simplicity, we do not consider transmitter impairments in the remote signal $\mathbf{x}$ as

these will typically lie far below the noise floor caused by $\mathbf{n}_{\text{eff}}$. As can be seen from (7), the elements of $\mathbf{n}_{\text{eff}}$ will always be *spatially correlated*, since they are linear combinations of the elements of $\mathbf{n}_{\text{t}}$ and $\mathbf{n}_{\text{c}}$.

III. FD-MIMO Testbed and Measurement Setup

Our 2×2 FD-MIMO node, which is described in more detail in [4], is based on the National Instruments PXIe platform with NI 5791R RF modules providing the conversion from complex baseband samples to the analog RF domain. Two RF modules are required per MIMO channel: one for transmission and reception and one to generate the cancelation signal. Each of the two RF modules is equipped with a circulator, which provides approximately 15 dB of isolation between the transmitter and the receiver. One omnidirectional antenna with a 2 dBi gain is used per chain and the spacing between the two antennas is 15 cm. The most important transmitter impairment that limits suppression in FD systems is phase noise [5]. In our testbed, the carrier is shared between all transmitter chains, hence, in principle, they should experience *identical* phase noise. However, in practice they experience only *highly correlated* phase noise, because of slight differences in the self-interference and the cancelation signal path lengths. The complex baseband samples are generated in MATLAB and are transferred via Ethernet to the PXIe platform. The PXIe platform, in turn, records the received baseband samples and sends them back to MATLAB.

The measurements are performed as follows. We operate in the 2.45 GHz band with a 0 dBm transmit power. Each OFDM frame consists of 40 OFDM symbols with QPSK modulation, with a 10 MHz bandwidth split into 256 subcarriers. We transmit $N_f = 100$ OFDM frames $\mathbf{x}_{\text{t}}$ and the corresponding cancelation signals $\mathbf{x}_{\text{c}}$ and we record the residual self-interference signal for each receiver. We concatenate the resulting residual self-interference signals into a $2\times N$ matrix, denoted by $\mathbf{N}$, where $N = N_f \cdot N_s$ and N_s is the number of time domain samples contained in each OFDM frame (in our case $N_s = 12'240$, because we use a cyclic prefix of 50 samples). All measurements are performed in the absence of the remote signal $\mathbf{x}$, since our aim is to measure and characterize $\mathbf{n}_{\text{eff}}$. We note that the overall RF suppression is more than 65 dB, so we are able to operate our receiver at its maximum sensitivity when measuring $\mathbf{n}_{\text{eff}}$. This means that the power of the self-interference is reduced to a level at which a remote signal $\mathbf{x}$, if it were present, could be received with no impact on the sensitivity of the receiver. The channels $\mathbf{H}_{\text{t}}$ and $\mathbf{H}_{\text{c}}$ are estimated using a long estimation sequence to minimize the estimation error. We thus ensure that (6) holds and that the traces of $\mathbf{x}_{\text{t}}$ left in the residual signals are minimal.

IV. Characterization of effective noise

A. Statistical metrics

The spatial correlation of $\mathbf{n}_{\text{eff}}$ along the two antennas is given by the covariance matrix $\mathbf{K}$, which is defined as $\mathbf{K} \triangleq \mathbb{E}\left[\left(\mathbf{n}_{\text{eff}} - \mathbb{E}[\mathbf{n}_{\text{eff}}]\right)\left(\mathbf{n}_{\text{eff}} - \mathbb{E}[\mathbf{n}_{\text{eff}}]\right)^H\right]$. We estimate $\mathbf{K}$ as

$$\hat{\mathbf{K}} = \frac{1}{N}\left(\mathbf{N} - \mathbf{m}\right)\left(\mathbf{N} - \mathbf{m}\right)^H, \tag{8}$$

where $\mathbf{m}_i = \frac{1}{N}\sum_{k=1}^{N}\mathbf{N}_{i,k},\ i = 1,2$, is the ML estimate of $\mathbb{E}[\mathbf{n}_{\text{eff}}]$. Moreover, we compute an estimate of the auto-correlation of each element of $\mathbf{n}_{\text{eff}}$ in time as

$$\hat{\mathbf{R}}_{i,j} = \begin{cases} \sum_{k=0}^{N-j-1}\mathbf{N}_{i,j+k}\mathbf{N}_{i,k}^*, & j \geq 0, \\ \hat{\mathbf{R}}_{i,-j}^*, & j < 0, \end{cases} \tag{9}$$

with $i = 1,2$, and $j = -N_f \cdot N_s + 1, \ldots, N_f \cdot N_s - 1$. Furthermore, we fit some probability distributions to $\mathbf{N}$ in order to estimate the statistics of $\mathbf{n}_{\text{eff}}$ in the time and in the frequency domain. Finally, we briefly comment on the correlation between $\Re(\mathbf{n}_{\text{eff}})$ and $\Im(\mathbf{n}_{\text{eff}})$, and on the circularity of $\mathbf{n}_{\text{eff}}$ by using the pseudo-variance for each chain i, which is defined as $\tau_i^2 \triangleq \mathbb{E}\left[\mathbf{n}_{\text{eff},i}^2\right]$ and estimated as $\hat{\tau}_i^2 = \frac{1}{N}\sum_{j=1}^{N}\mathbf{N}_{i,j}^2$. A smaller pseudo-variance indicates a more circular complex random variable.

B. Results

1) Spatial Covariance Matrices: We computed the following spatial covariance matrices for the effective noise in the time domain

$$\hat{\mathbf{K}}_{\text{time}} = \begin{bmatrix} 0.0067 & -0.0013 - 0.0031i \\ -0.0013 + 0.0031i & 0.0053 \end{bmatrix}, \tag{10}$$

and in the frequency domain

$$\hat{\mathbf{K}}_{\text{freq}} = \begin{bmatrix} 0.0070 & -0.0013 - 0.0039i \\ -0.0013 + 0.0039i & 0.0057 \end{bmatrix}, \tag{11}$$

which both clearly indicate that the effective noise is spatially correlated.[1] In order to assess whether the correlation comes only from the channels $\mathbf{H}_{\text{t}}$ and $\mathbf{H}_{\text{c}}$, we performed the following experiment in MATLAB. We generated $\mathbf{n}_{\text{c}}$ and $\mathbf{n}_{\text{t}}$ with i.i.d. elements and applied (7) with the estimated channels $\mathbf{H}_{\text{t}}$ and $\mathbf{H}_{\text{c}}$. The resulting effective noise is significantly less correlated than the effective noise that we observe, which suggests that $\mathbf{n}_{\text{t}}$ and $\mathbf{n}_{\text{c}}$ are inherently correlated.

2) Autocorrelations: In Fig. 1 we plot a normalized version of $|\hat{\mathbf{R}}_{1,j}|$ in the time domain. We observe that the autocorrelation decays very quickly with increasing lag j. Moreover, as can be seen in Fig. 2, where a normalized version of $|\hat{\mathbf{R}}_{1,j}|$ in the frequency domain is plotted, there is no visible correlation across the carriers. We note that $|\hat{\mathbf{R}}_{2,j}|$ (not plotted here) shows the same behavior both in the time and in the frequency domain.

[1]The covariance matrix is invariant with respect to the FFT operation. However, the correlation in (10) is slightly different from the one in (11) because the FFT operation is performed in blocks of N samples of each row of $\mathbf{N}$, and not over each entire row of $\mathbf{N}$.

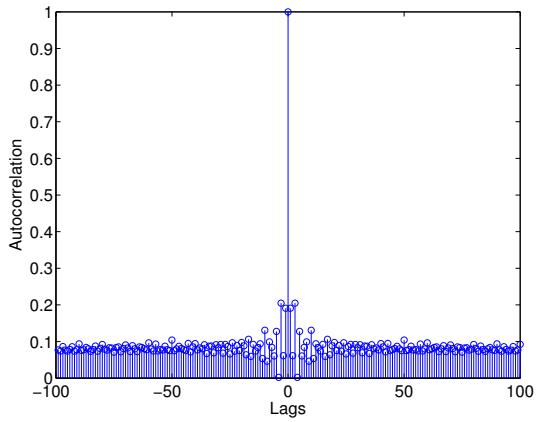

Fig. 1. Magnitude of the autocorrelation of $\mathbf{N}_{1,j}$ in the time domain.

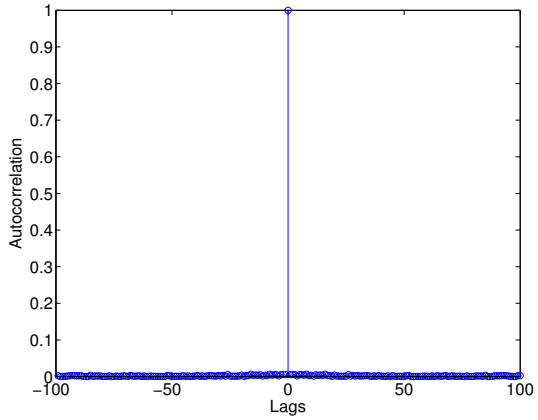

Fig. 2. Magnitude of the autocorrelation of $\mathbf{N}_{1,j}$ in the frequency domain.

3) Histograms: In Fig. 3, we present an indicative histogram of $\Re(\mathbf{N}_{1,j})$, along with a normal distribution fitted to our measurements. Interestingly, we find that a normal distribution does not represent our time domain effective noise accurately. Instead, we found that the *t location-scale* distribution can very accurately represent our data. The t location-scale distribution has three parameters, namely, μ, which is the location parameter, σ^2, which is the scaling parameter, and ν, which is the degrees of freedom parameter. For $\nu \to \infty$, the distribution becomes Gaussian. A fitted t location-scale distribution is also shown in Fig. 3. We know from our measurements that the effective noise in the time domain is a zero-mean stochastic process. Let us also assume that the effective noise samples in the time domain are i.i.d. Then, each effective noise sample in the frequency domain is a linear combination of zero-mean i.i.d. random variables, which, by the (Lyapunov) central limit theorem, converges to a Gaussian random variable. In Fig. 4 we see that the effective noise in the frequency domain is indeed well represented by a Gaussian distribution. We note that $\Im(\mathbf{N}_{1,j})$, $\Re(\mathbf{N}_{2,j})$, and $\Im(\mathbf{N}_{2,j})$, which are not plotted here, show the same behavior both in the time and in the frequency domain.

4) Correlation and circularity: In Fig. 5 and Fig. 6, we present histograms of $\mathbf{N}_{1,j}$ in the time and in the frequency

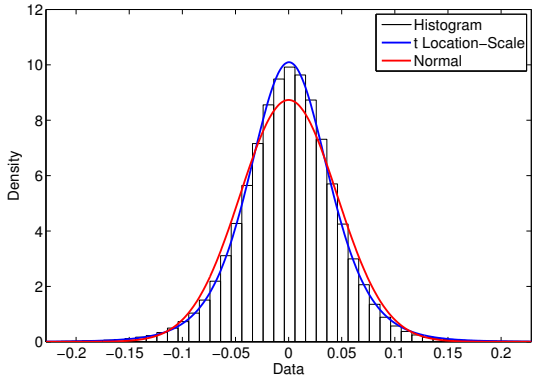

Fig. 3. Histogram of $\Re(\mathbf{N}_{1,j})$ measured in the time domain with fitted Gaussian distribution with $\mu \approx 0$ and $\sigma^2 = 0.0625$, and t location-scale distribution with $\mu \approx 0$, $\sigma^2 = 0.0571$, and $\nu = 14.57$.

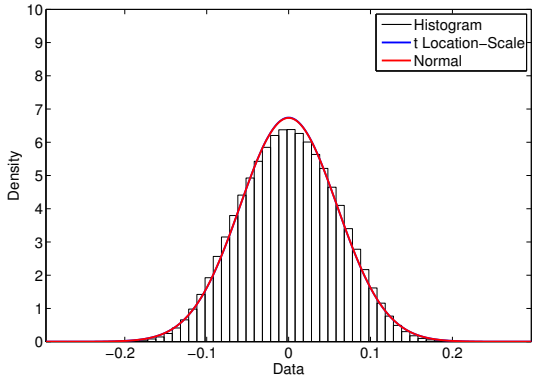

Fig. 4. Histogram of $\Re(\mathbf{N}_{1,j})$ measured in the frequency domain with fitted Gaussian distribution with $\mu \approx 0$ and $\sigma^2 = 0.0592$, and t location-scale distribution with $\mu \approx 0$, $\sigma^2 = 0.0591$, and $\nu \approx 523.71$.

domain. We observe that in the time domain the correlation between $\Re(\mathbf{n}_{\text{eff},1})$ and $\Im(\mathbf{n}_{\text{eff},1})$ is very apparent, while in the frequency domain this correlation disappears. Moreover, since in the frequency domain the real and imaginary parts of each element of $\mathbf{n}_{\text{eff}}$ are well approximated by a Gaussian random variable, we can also say that they are (approximately) independent. For the pseudo-variance, we have $\hat{\tau}_1^2 = 0.0009 + 0.0024i$ in the time domain and $\hat{\tau}_1^2 = -1.31 \cdot 10^{-5} + 2.35 \cdot 10^{-7} i$ in the frequency domain, indicating that in the frequency domain $\mathbf{n}_{\text{eff},1}$ is more circular.

V. Effect on ZF and ML Receivers

We perform simulations in order to compare the performance of the ZF and ML receivers under i.i.d. complex normal noise and under the recorded effective noise. The i.i.d. complex normal noise is generated in MATLAB, while for the effective noise we use the frequency domain noise samples $\mathbf{N}$ that we recorded using our testbed. More specifically, we simulate an OFDM system with QPSK modulation. Each frame consists of one OFDM symbol, which in turn contains 50 data symbols. Moreover, we apply the noise whitening method presented in [6] to combat the spatially correlated

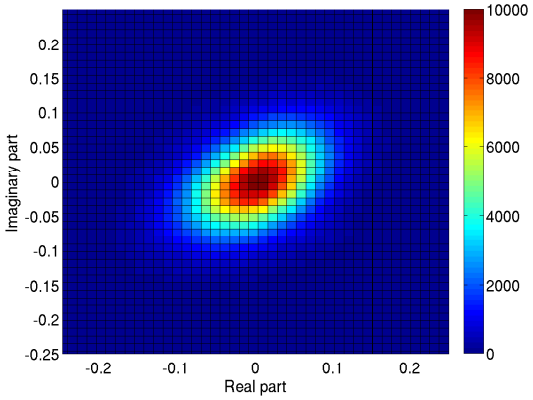

Fig. 5. Histogram of $\mathbf{N}_{1,j}$ in the time domain.

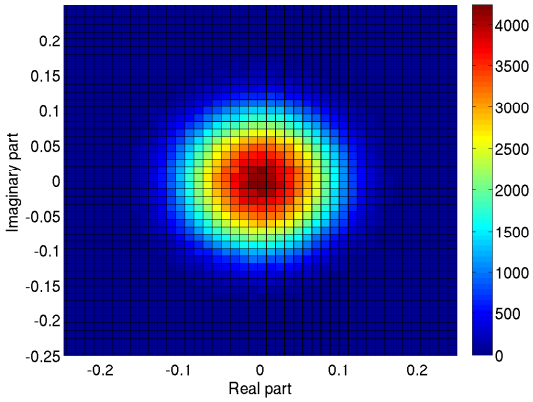

Fig. 6. Histogram of $\mathbf{N}_{1,j}$ in the frequency domain.

noise. The whitening method is based on pre-multiplying the received vector $\mathbf{y}$ and the channel matrix $\mathbf{H}$ with a whitening filter $\mathbf{W}$, where $\mathbf{W} = \mathbf{K}^{-1/2}$. We observe in our experiments that $\hat{\mathbf{K}}$ varies slightly from frame to frame. Ideally, one would like to use the $\hat{\mathbf{K}}$ that corresponds to each frame, but in a real-world scenario it is harder to accurately estimate $\hat{\mathbf{K}}$ because of the presence of the signal $\mathbf{x}$ of the remote node, which disturbs the parameter estimation. For this reason, we use the average $\hat{\mathbf{K}}$ which we calculated in Section III to perform whitening. The recorded effective noise $\mathbf{N}$ is normalized in such a way that, *after* noise whitening, it has a power equal to the generated i.i.d. complex normal noise for each SNR, where the power N_0 and the (per-antenna) SNR are defined as $N_0 = \frac{1}{2N}\|\mathbf{N}\|_{\mathrm{F}}^2$ and $\mathrm{SNR} = \frac{1}{N_0}$, respectively. The power N_0 is then spread equally across the antennas and across the real and imaginary dimensions. The recorded noise samples are randomly interleaved with respect to time in order to eliminate any time-correlation. However, we are careful to use noise samples from the same time instance for each receiver in order to maintain the spatial correlation. For our simulations, it is assumed that $\mathbf{H} \sim \mathcal{CN}(\mathbf{0}, \mathbf{I}_2)$.

In Fig. 7 we plot the frame error rate (FER) for the ZF and ML receivers under complex normal noise and under the recorded noise. We observe that the performance of both the ZF and ML receivers is degraded with respect to the case

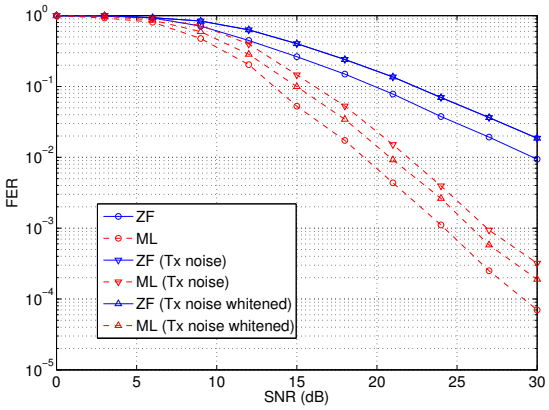

Fig. 7. FER of ZF and ML receivers under i.i.d. complex normal and measured frequency domain effective noise for an OFDM FD-MIMO system.

where we have complex normal noise when noise whitening is not performed. Moreover, we observe that noise whitening does indeed improve the performance of the ML receiver, while it does not affect the ZF receiver, as expected [6].

VI. Conclusion

In this paper, we measured the residual self-interference on an FD-MIMO testbed. Interestingly, the residual self-interference of our testbed in the time domain is not well described by a Gaussian distribution. After the FFT function performed by the OFDM receiver, the distribution of the residual self-interference at each receiver is well approximated by the usual *circular symmetric complex normal* distribution, but the noise is spatially correlated across the receiver chains. We also studied the effect of residual self-interference on some MIMO receivers and we applied a noise whitening method to improve their performance under spatially correlated noise.

Acknowledgment

This work was supported by the Swiss NSF under project 200021_146753.

References

[1] S. Chen, M. A. Beach, and J. P. McGeehan, "Division-free duplex for wireless applications," *Electronics Letters*, vol. 34, no. 2, pp. 147–148, Jan. 1998.

[2] D. Bharadia, E. McMilin, and S. Katti, "Full duplex radios," in *ACM SIGCOMM'13*, Aug. 2013.

[3] M. Duarte, C. Dick, and A. Sabharwal, "Experiment-driven characterization of full-duplex wireless systems," *IEEE Trans. Wireless Commun.*, vol. 11, no. 12, pp. 4296–4307, 2012.

[4] A. Balatsoukas-Stimming, P. Belanovic, K. Alexandris, and A. Burg, "On self-interference suppression methods for low-complexity full-duplex MIMO," *Asilomar Conf. on Signals, Systems, and Computers*, Nov. 2013.

[5] A. Sahai, G. Patel, C. Dick, and A. Sabharwal, "On the impact of phase noise on active cancellation in wireless full-duplex," 2013, *IEEE Trans. on Vehicular Techn.*, vol. 62, no. 9, pp. 4494–4519, Nov. 2013.

[6] C. Studer, M. Wenk, and A. Burg, "MIMO transmission with residual transmit-RF impairments," in *Int. Workshop Smart Antennas*, Feb. 2010, pp. 189–196.

[7] M. Vehkapera, T. Riihonen, and R. Wichman, "Asymptotic analysis of full-duplex bidirectional MIMO link with transmitter noise," *IEEE Int. Symp. Pers. Indoor and Mob. Radio Commun.*, pp. 1265–1270, Sep. 2013.

[8] D. W. Bliss, T. M. Hancock, and P. Schniter, "Hardware phenomenological effects on cochannel full-duplex MIMO relay performance," *Asilomar Conf. on Signals, Systems, and Computers*, pp. 34-39, Nov. 2012.